QCD at finite chemical potential in and out-of equilibrium

Elena Bratkovskaya

(GSI Darmstadt & Uni. Frankfurt)

Olga Soloveva, Pierre Moreau, Lucia Oliva, Taesoo Song, Wolfgang Cassing

9th International Conference on New Frontiers in Physics (ICNFP 2020)

Kolymbari, Greece, 4-12 September 2020

The ‚holy grail‘ of heavy-ion physics:

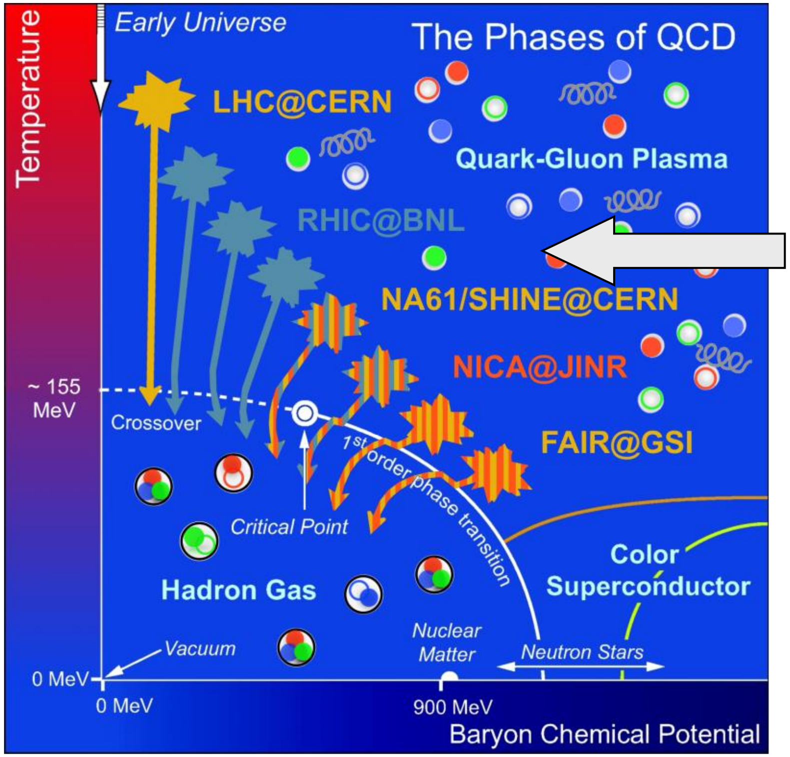

The phase diagram of QCD

- Study of the phase transition from hadronic to partonic matter – Quark-Gluon-Plasma
- Search for possible critical point
- Search for signatures of chiral symmetry restoration
- Study of the in-medium properties of hadrons at high baryon density and temperature

Our goal: to study the properties of strongly interacting matter created in heavy-ion collisions on a microscopic basis

Theory: QCD + many body theory + microscopic transport theory

Realization: dynamical transport approach → PHSD

Theory: lattice QCD data for $\mu_B = 0$ and finite $\mu_B > 0$

- Deconfinement phase transition from hadron gas to QGP with increasing T and μ_B

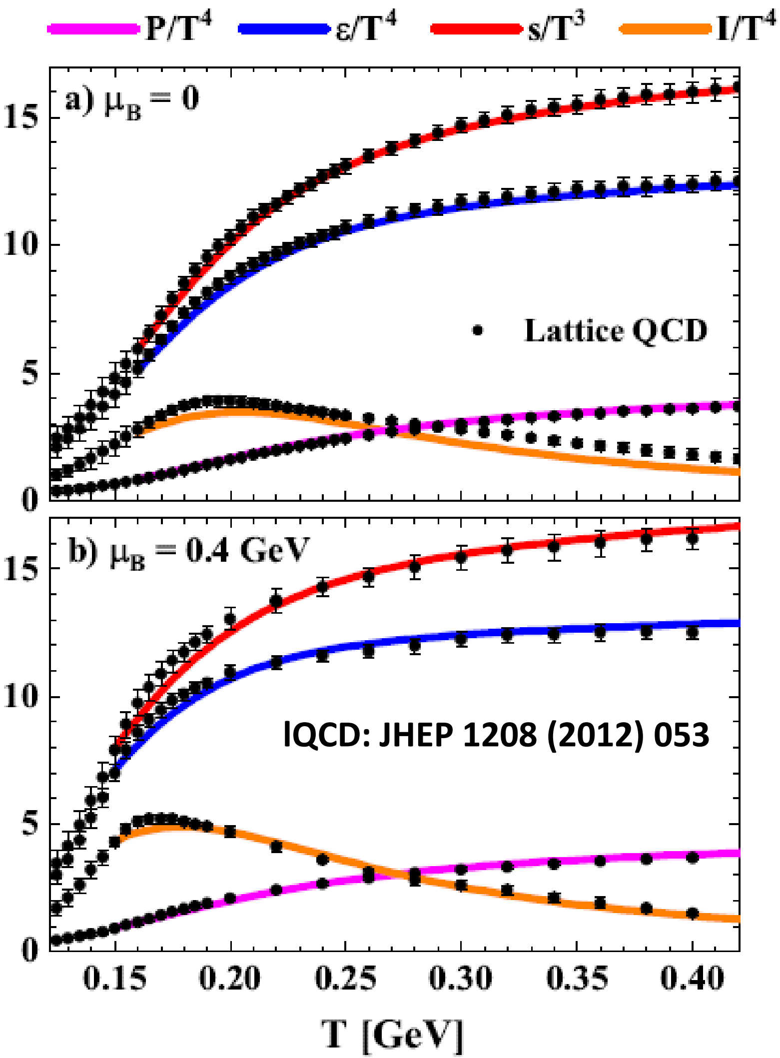

lQCD: J. Guenther et al., Nucl. Phys. A 967 (2017) 720

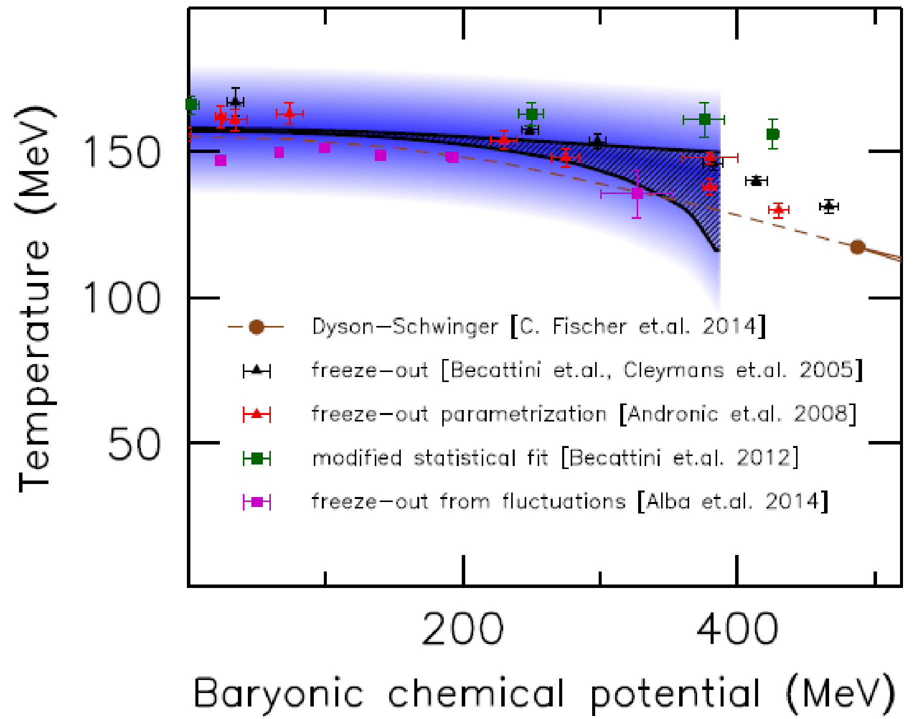

➔ Lattice QCD results: up to $\mu_B < 400\ MeV$:
Crossover: hadron gas → QGP

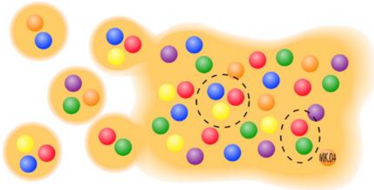

Degrees-of-freedom of QGP

For the microscopic transport description of the system one needs to know all degrees of freedom as well as their properties and interactions!

❖ lQCD gives QGP EoS at finite μ_B

! need to be interpreted in terms of degrees-of-freedom

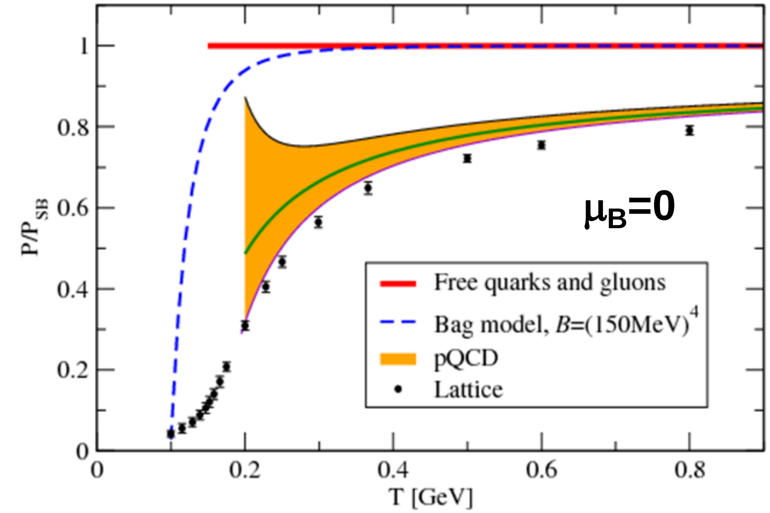

Non-perturbative QCD ← pQCD

pQCD:

- ❑ weakly interacting system
- ❑ massless quarks and gluons

Thermal QCD
= QCD at high parton densities:

- ❑ strongly interacting system
- ❑ massive quarks and gluons

➔ quasiparticles
= effective degrees-of-freedom

How to learn about the degrees-of-freedom of QGP from HIC?
➔ microscopic transport approaches
➔ comparison to HIC experiments

DQPM (T, μ_q)

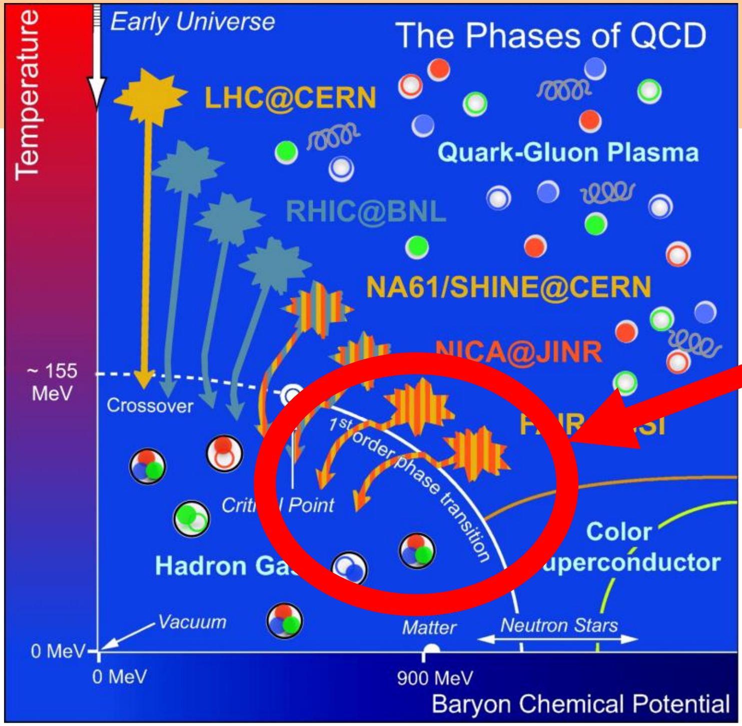

finite μ_q

Dynamical QuasiParticle Model (DQPM)

DQPM – effective model for the description of non-perturbative (strongly interacting) QCD based on lQCD EoS

Degrees-of-freedom: strongly interacting dynamical quasiparticles - quarks and gluons

Theoretical basis :

- ‚resummed' single-particle Green's functions ➔ quark (gluon) propagator (2PI) :

gluon propagator: $\Delta^{-1} = P^2 - \Pi$	&	quark propagator $G_q^{-1} = P^2 - \Sigma_q$
gluon self-energy: $\Pi = M_g^2 - i2\gamma_g\omega$	&	quark self-energy: $\Sigma_q = M_q^2 - i2\gamma_q\omega$

Properties of the quasiparticles are specified by scalar complex self-energies:

$Re\Sigma_q$: thermal masses (M_g, M_q); $Im\Sigma_q$: interaction widths (γ_g, γ_q)

➔ spectral functions $\rho_q = -2ImG_q$

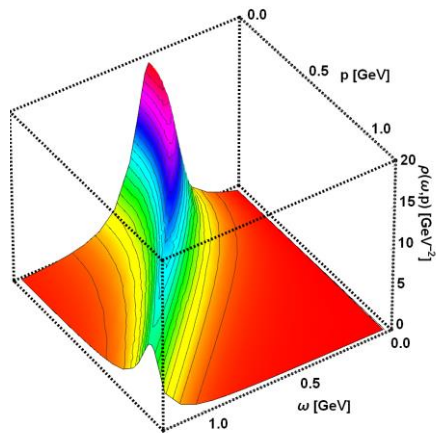

- introduce an ansatz (HTL; with few parameters) for the (T, μ_B) dependence of masses/widths
- evaluate the QGP thermodynamics in equilibrium using the Kadanoff-Baym theory
- fix DQPM parameters by comparison to the entropy density s, pressure P, energy density ε from DQPM to lQCD at μ_B=0

A. Peshier, W. Cassing, PRL 94 (2005) 172301; W. Cassing, NPA 791 (2007) 365: NPA 793 (2007), H. Berrehrah et al, Int.J.Mod.Phys. E25 (2016) 1642003; P. Moreau et al., PRC100 (2019) 014911; O. Soloveva et al., PRC101 (2020) 045203

Parton properties

- Modeling of the quark/gluon masses and widths (inspired by HTL calculations)

Masses:

$$M^2_{q(\bar q)}(T,\mu_B) = \frac{N_c^2-1}{8N_c} g^2(T,\mu_B)\left(T^2+\frac{\mu_q^2}{\pi^2}\right)$$

$$M^2_g(T,\mu_B) = \frac{g^2(T,\mu_B)}{6}\left(\left(N_c+\frac{1}{2}N_f\right)T^2+\frac{N_c}{2}\sum_q\frac{\mu_q^2}{\pi^2}\right)$$

Widths:

$$\gamma_{q(\bar q)}(T,\mu_B) = \frac{1}{3}\frac{N_c^2-1}{2N_c}\frac{g^2(T,\mu_B)T}{8\pi}\ln\left(\frac{2c}{g^2(T,\mu_B)}+1\right)$$

$$\gamma_g(T,\mu_B) = \frac{1}{3}N_c\frac{g^2(T,\mu_B)T}{8\pi}\ln\left(\frac{2c}{g^2(T,\mu_B)}+1\right)$$

→ **DQPM :**
only one parameter (c = 14.4) + (T,μ_B)- dependent coupling constant has to be determined from lattice results

- **Coupling:** input: lQCD entropy density as a function of temperature for μ_B
  → Fit to lattice data at μ_B=0 with

$$g^2(s/s_{SB}) = d\left((s/s_{SB})^e-1\right)^f$$

$$s_{SB}^{QCD} = 19/9\pi^2T^3$$

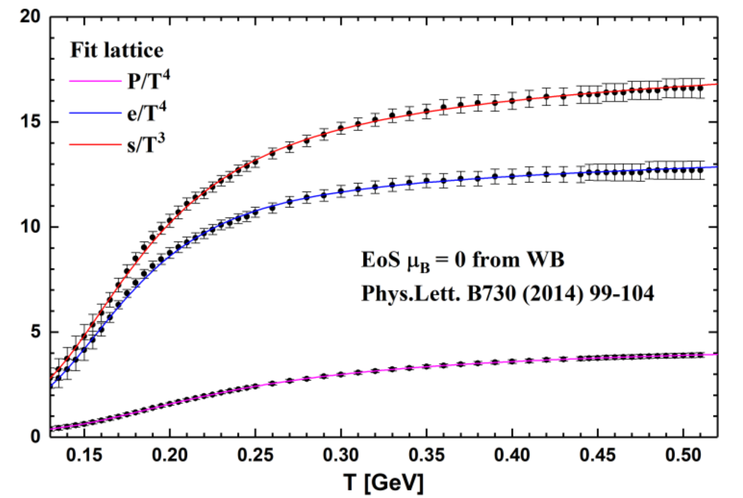

H. Berrehrah et al, PRC 93 (2016) 044914, Int.J.Mod.Phys. E25 (2016) 1642003,

DQPM at finite (T, μ_q): scaling hypothesis

- **Scaling hypothesis for the effective temperature T***
  for $N_f = N_c = 3$

$$\mu_u = \mu_d = \mu_s = \mu_q$$

$$\boxed{T^{*2} = T^2 + \frac{\mu_q^2}{\pi^2}}$$

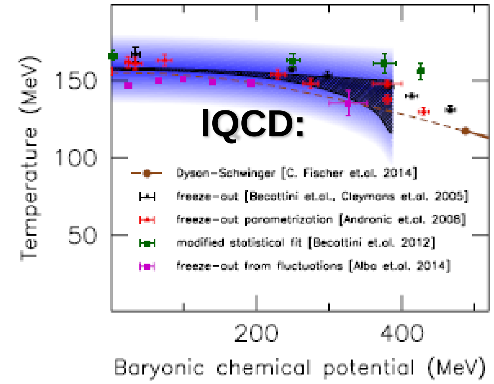

- **Coupling:**

$$g(T/T_c(\mu=0)) \longrightarrow g(T^\star/T_c(\mu))$$

- **Critical temperature $T_c(\mu_q)$:**
  obtained by assuming a constant energy density ε for the system at $T=T_c(\mu_q)$, where ε at $T_c(\mu_q=0)=156$ GeV is fixed by lQCD at $\mu_q=0$

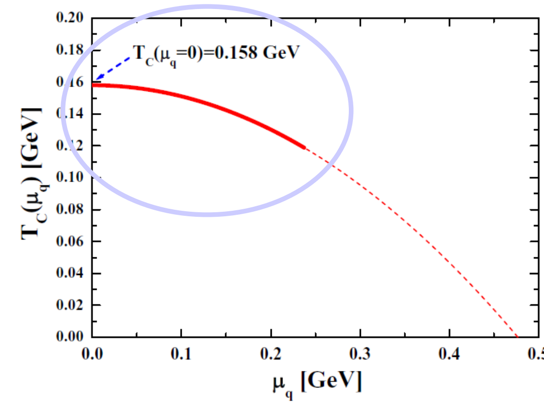

$$\boxed{\frac{T_c(\mu_q)}{T_c(\mu_q=0)} = \sqrt{1-\alpha\,\mu_q^2} \approx 1 - \alpha/2\,\mu_q^2 + \cdots}$$

$$\alpha \approx 8.79\ \mathrm{GeV}^{-2}$$

! Consistent with lattice QCD:

$$\frac{T_c(\mu_B)}{T_c} = 1 - \kappa\left(\frac{\mu_B}{T_c}\right)^2 + \cdots$$

lQCD: C. Bonati et al., PRC90 (2014) 114025

lQCD $\kappa = 0.013(2)$ $\longleftrightarrow$ $\kappa_{DQPM} \approx 0.0122$

H. Berrehrah et al, PRC 93 (2016) 044914, Int.J.Mod.Phys. E25 (2016) 1642003,

DQPM: parton properties

- Coupling as a function of (T, μ_B)

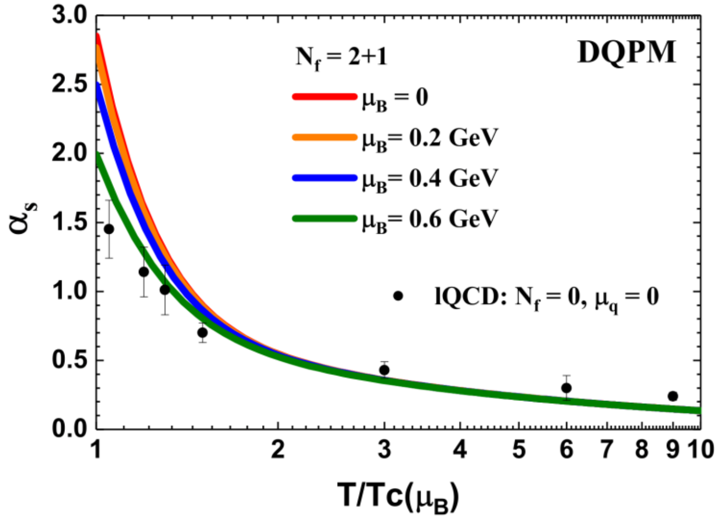

➔ **Lorentzian spectral function:**

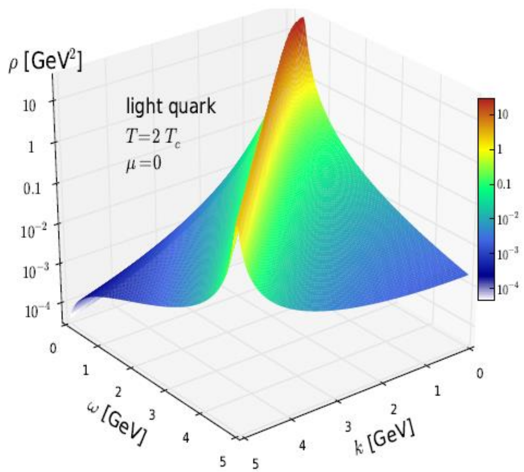

- Masses and widths as a function of (T, μ_B)

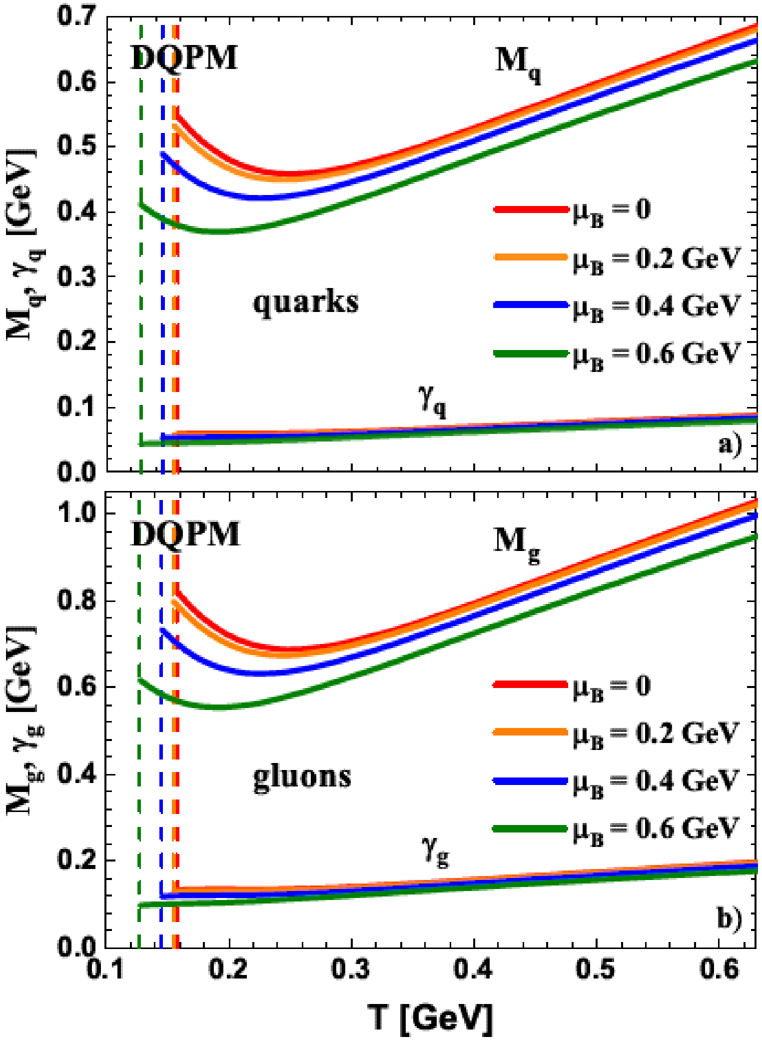

P. Moreau et al., PRC100 (2019) 014911

DQPM thermodynamics at finite (T, μ_q)

- **Entropy and baryon density** in the quasiparticle limit (G. Baym 1998):

$$s^{dqp} = - \int \frac{d\omega}{2\pi} \frac{d^3p}{(2\pi)^3} \left[d_g \frac{\partial n_B}{\partial T} \left(\mathrm{Im}(\ln -\Delta^{-1}) + \mathrm{Im}\,\Pi\, \mathrm{Re}\,\Delta \right) + \sum_{q=u,d,s} d_q \frac{\partial n_F(\omega-\mu_q)}{\partial T} \left(\mathrm{Im}(\ln -S_q^{-1}) + \mathrm{Im}\,\Sigma_q\, \mathrm{Re}\,S_q \right) + \sum_{\bar q=\bar u,\bar d,\bar s} d_{\bar q} \frac{\partial n_F(\omega+\mu_q)}{\partial T} \left(\mathrm{Im}(\ln -S_{\bar q}^{-1}) + \mathrm{Im}\,\Sigma_{\bar q}\, \mathrm{Re}\,S_{\bar q} \right) \right]$$

$$n^{dqp} = - \int \frac{d\omega}{2\pi} \frac{d^3p}{(2\pi)^3} \left[\sum_{q=u,d,s} d_q \frac{\partial n_F(\omega-\mu_q)}{\partial \mu_q} \left(\mathrm{Im}(\ln -S_q^{-1}) + \mathrm{Im}\,\Sigma_q\, \mathrm{Re}\,S_q \right) + \sum_{\bar q=\bar u,\bar d,\bar s} d_{\bar q} \frac{\partial n_F(\omega+\mu_q)}{\partial \mu_q} \left(\mathrm{Im}(\ln -S_{\bar q}^{-1}) + \mathrm{Im}\,\Sigma_{\bar q}\, \mathrm{Re}\,S_{\bar q} \right) \right]$$

Blaizot, Iancu, Rebhan, Phys. Rev. D 63 (2001) 065003

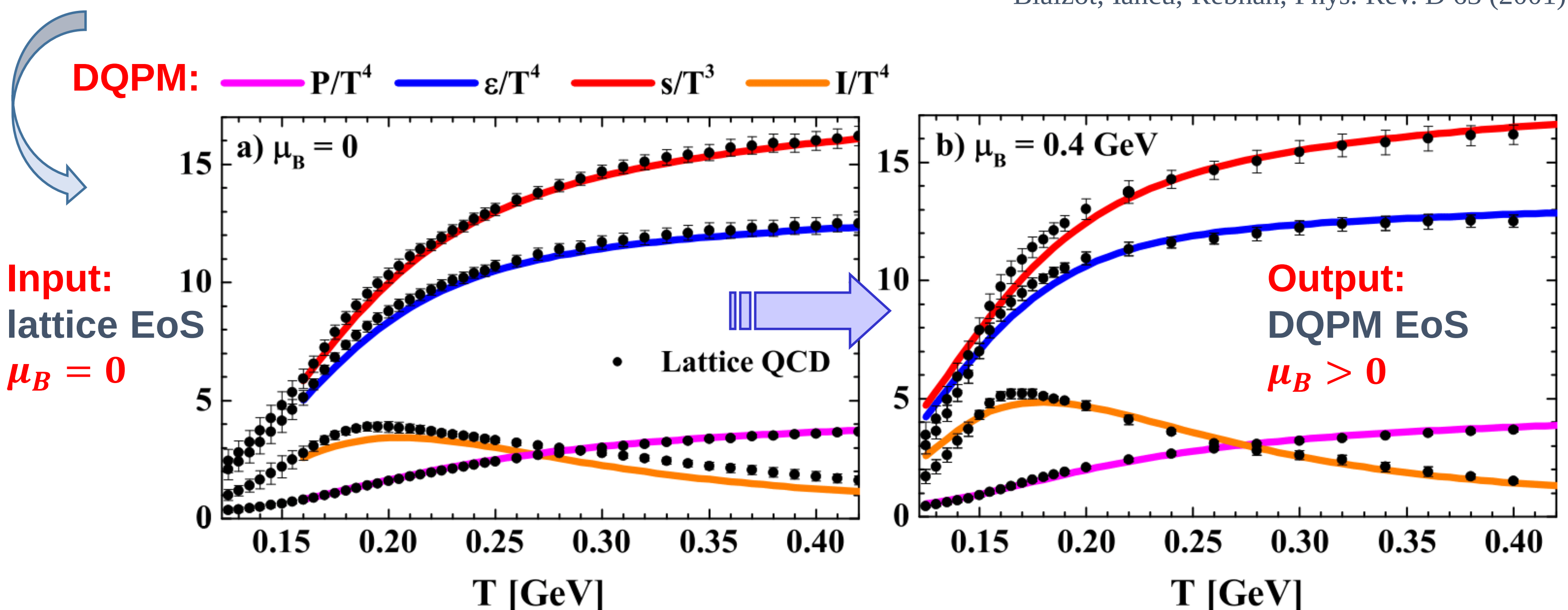

lQCD: JHEP 1208 (2012) 053

DQPM: Mean-field potential for quasiparticles

Space-like part of energy-momentum tensor $T_{\mu\nu}$ defines the potential energy density:

$$V_p(T,\mu_q) = T^{00}_{g-}(T,\mu_q) + T^{00}_{q-}(T,\mu_q) + T^{00}_{\bar{q}-}(T,\mu_q)$$

space-like gluons **space-like quarks+antiquarks**

➔ **mean-field scalar potential (1PI) for quarks and gluons (U_q, U_g) vs scalar density ρ_S:**

$$U_s(\rho_s) = \frac{dV_p(\rho_s)}{d\rho_s}$$

$$U_q = U_s, \quad U_g \sim 2U_s$$

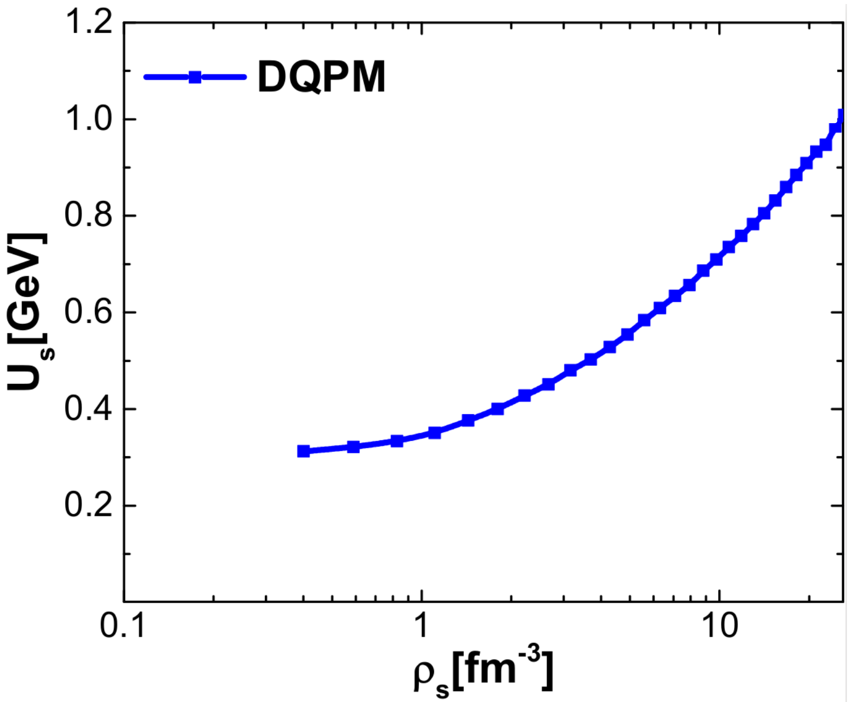

- **Quasiparticle potentials (U_q, U_g) are repulsive**

➔ **the force acting on a quasiparticle j:**

$$F \sim M_j/E_j \nabla U_s(x) = M_j/E_j\ dU_s/d\rho_s\ \nabla\rho_s(x)$$

$$j = g, q, \bar{q}$$

➔ **accelerates particles**

Cassing, NPA 791 (2007) 365: NPA 793 (2007)

Partonic interactions: matrix elements

DQPM partonic cross sections → leading order diagrams

- **Propagators for massive bosons and fermions:**

$$= -i\delta_{ab}\frac{g^{\mu\nu} - q^\mu q^\nu / M_g^2}{q^2 - M_g^2 + 2i\gamma_g q_0}$$

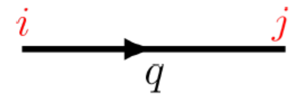

$$= i\delta_{ij}\frac{\not{q} + M_q}{q^2 - M_q^2 + 2i\gamma_q q_0}$$

qq' → qq' scattering

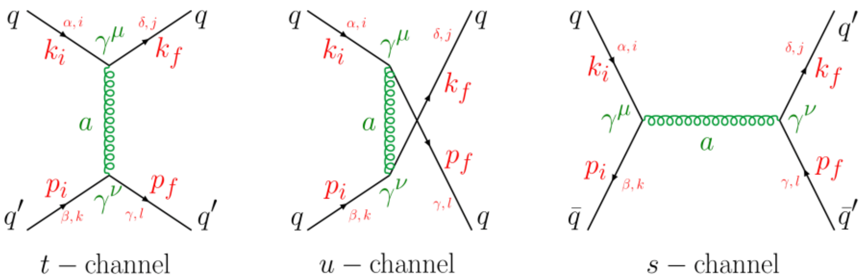

gq → gq scattering

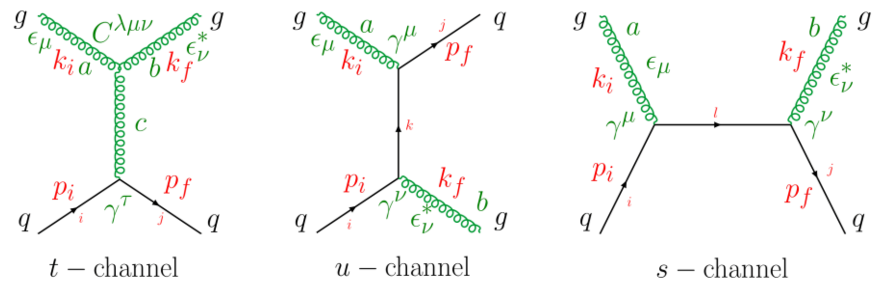

gg→ gg scattering

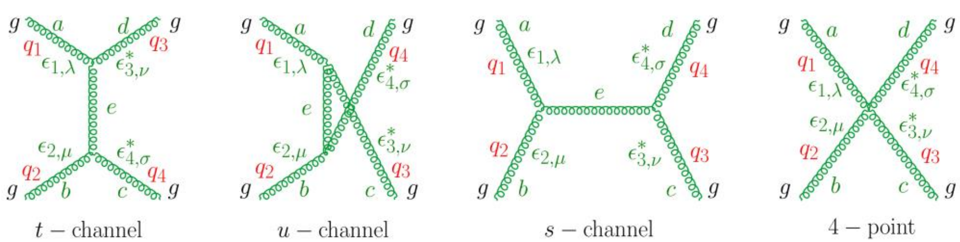

H. Berrehrah et al, PRC 93 (2016) 044914, Int.J.Mod.Phys. E25 (2016) 1642003, → **P. Moreau et al., PRC100 (2019) 014911**

Differential cross sections

□ **On-shell:**

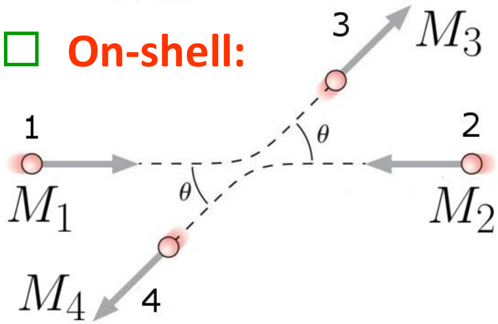

Initial masses: pole masses
Final masses: pole masses

□ **Off-shell:**

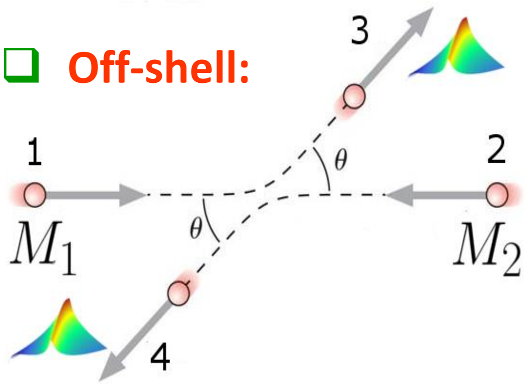

Initial masses: pole masses
Final masses: integrated over spectral functions

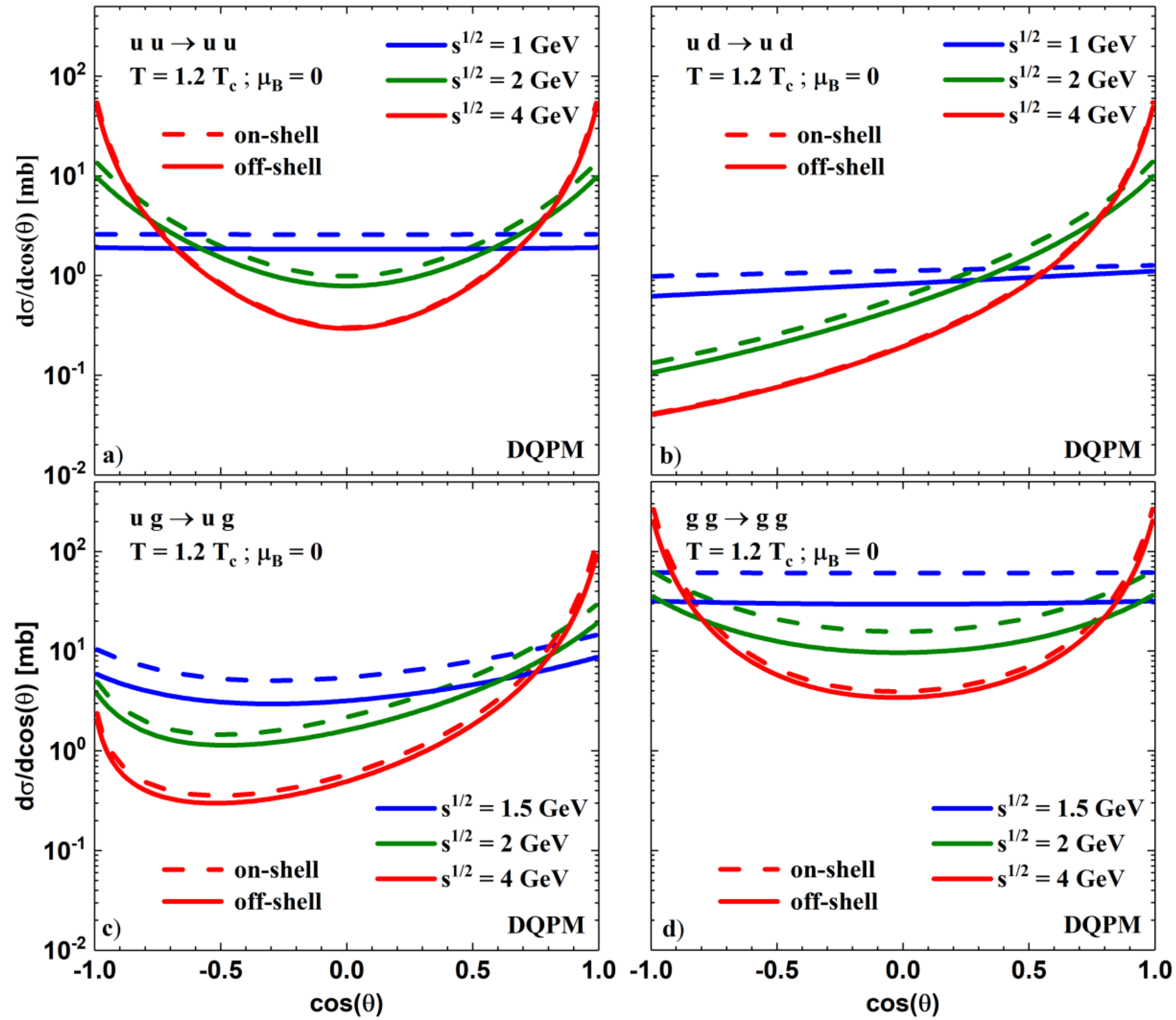

- **At lower s: off-shell σ < on -shell σ since $\omega_3 + \omega_4 < \sqrt{s}$**

P. Moreau et al., PRC100 (2019) 014911

QGP near equilibrium

DQPM (T, μ_q) :

transport properties at finite (T, μ_q)

Transport coefficients: shear viscosity η

- **Relaxation Time Approximation**

$$\eta^{\mathrm{RTA}}(T,\mu_B)=\frac{1}{15T}\sum_{i=q,\bar{q},g}\int\frac{d^3p}{(2\pi)^3}\frac{\mathbf{p}^4}{E_i^2}\boxed{\tau_i(\mathbf{p},T,\mu_B)}\,d_i(1\pm f_i)f_i$$

$$1)\tau_i(\mathbf{p},T,\mu_B)=\frac{1}{\Gamma_i(\mathbf{p},T,\mu_B)}$$

$$2)\tau_i(T,\mu_B)=\frac{1}{2\gamma_i(T,\mu_B)},$$

η/s versus (T,μ_B)

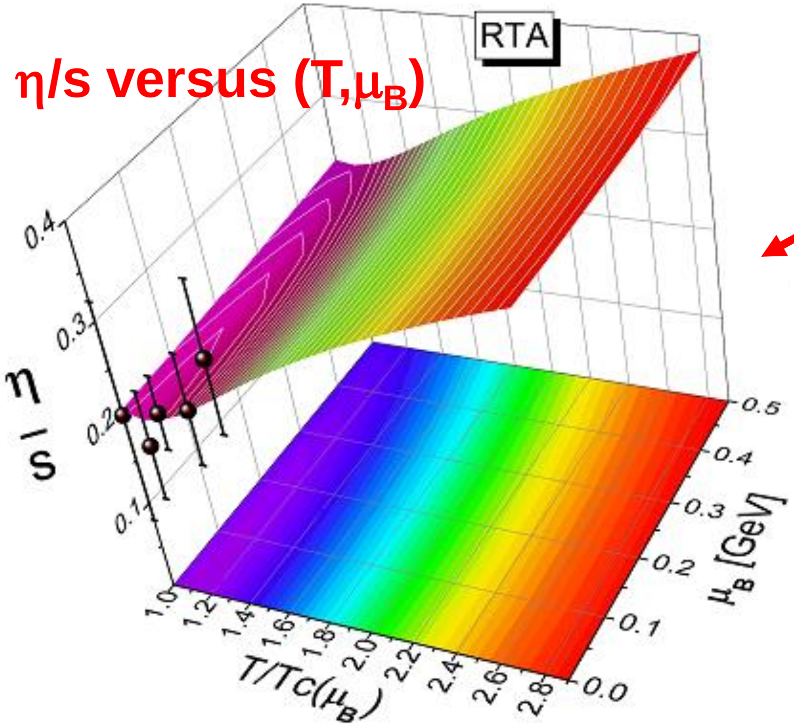

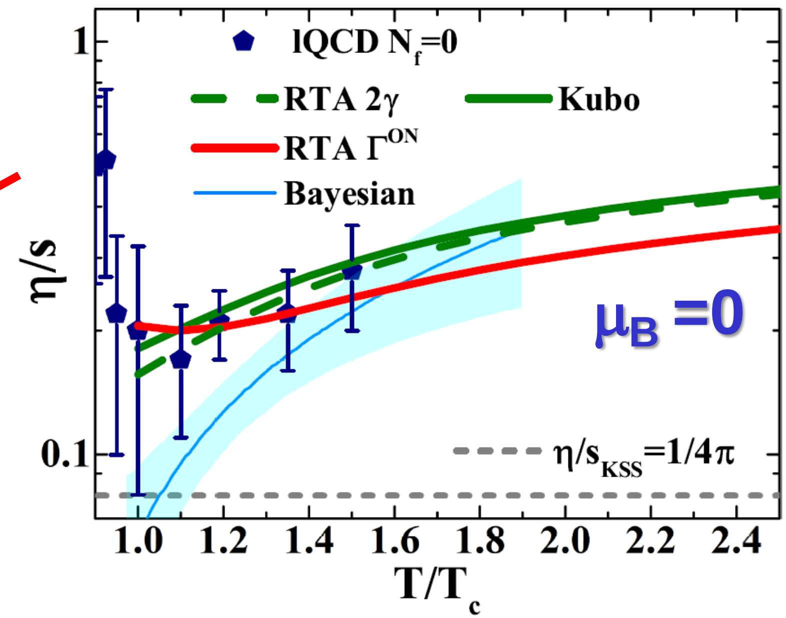

Hydro: Bayesian analysis, S. Bass et al. , NPA967 (2017) 67
Kovtun-Son-Starinets bound : $(\eta/s)_{KSS} = 1/(4\pi)$

- Very weak dependence of shere viscosity on μ_B

Lattice QCD: N. Astrakhantsev et al, JHEP 1704 (2017) 101

P. Moreau et al., PRC100 (2019) 014911; O. Soloveva et al., PRC110 (2020) 045203

Transport coefficients: bulk viscosity ζ

- **Relaxation Time Approximation**

Relaxation times

$$\zeta^{\mathrm{RTA}}(T,\mu_B) = \frac{1}{9T}\sum_{i=q,\bar{q},g}\int \frac{d^3p}{(2\pi)^3}\boxed{\tau_i(\mathbf{p},T,\mu_B)}$$

From DQPM parametrization

$$\frac{d_i(1\pm f_i)f_i}{E_i^2}\left(\mathbf{p}^2 - 3c_s^2\left(E_i^2 - T^2\frac{dm_i^2}{dT^2}\right)\right)^2$$

Speed of sound

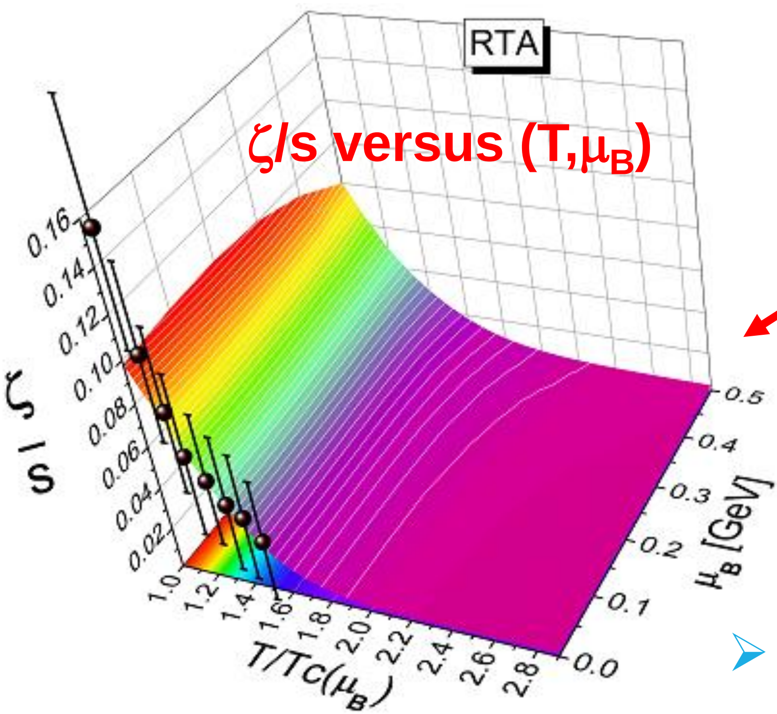

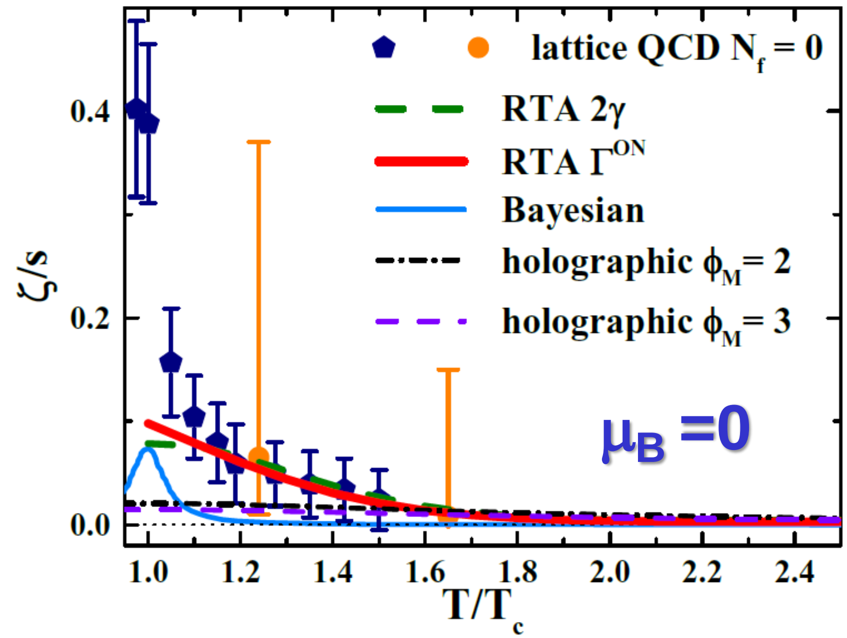

Lattice: Phys.Rev. D98 (2018) 054515

- **Very weak dependence of bulk viscosity on μ_B**

P. Moreau et al., PRC100 (2019) 014911; O. Soloveva et al., PRC110 (2020) 045203

Transport coefficients: electric conductivity σ_e/T

σ_0 ➔ Probe of electric properties of the QGP

η/s versus (T,μ_B)

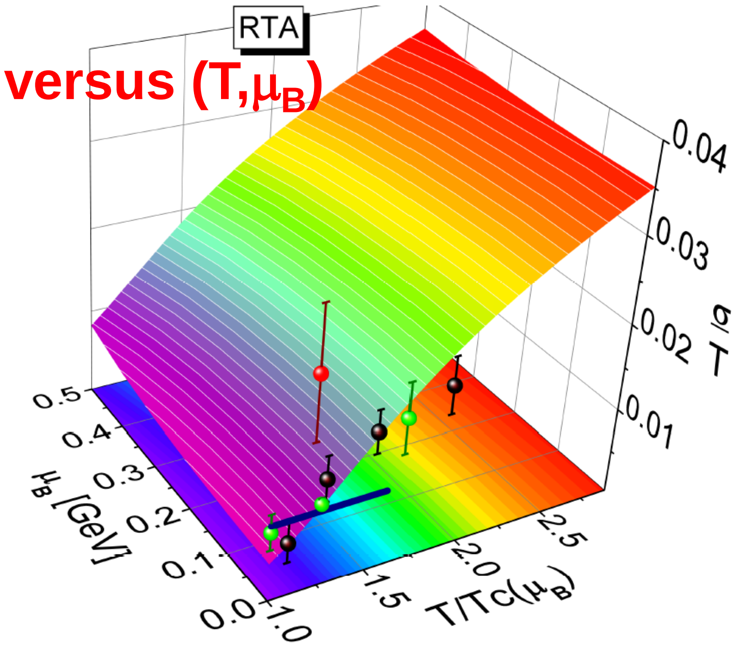

- **Relaxation Time Approximation**

$$\sigma_0^{\mathrm{RTA}}(T,\mu_B) = \frac{e^2}{3T} \sum_{i=q,\bar{q}} q_i^2 \int \frac{d^3p}{(2\pi)^3} \frac{\mathbf{p}^2}{E_i^2} \boxed{\tau_i(\mathbf{p},T,\mu_B)} d_i(1-f_i)f_i$$

Cf. talk by Pavel Buividovich

- **the QCD matter even at T~ T_c is a much better electric conductor than Cu or Ag (at room temperature) by a factor of 500 !**

Exp. observables – photon and dilepton spectra

- **Photon emission: rates at q_0→0 are related to electric conductivity σ_0**

$$q_0 \frac{dR}{d^4x\, d^3q}\bigg|_{q_0\to 0} = \frac{T}{4\pi^3}\sigma_0$$

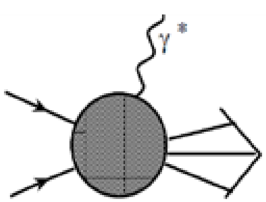

Review: H. Berrehrah et al. Int.J.Mod.Phys. E25 (2016) 1642003

QGP:
in-equilibrium → off-equilibrium

Parton-Hadron-String-Dynamics (PHSD)

PHSD is a non-equilibrium microscopic transport approach for the description of strongly-interacting hadronic and partonic matter created in heavy-ion collisions

Dynamics: based on the solution of generalized off-shell transport equations derived from Kadanoff-Baym many-body theory

Initial A+A collision

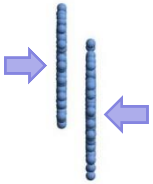

Partonic phase

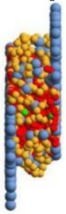

Hadronization

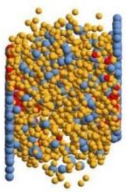

Hadronic phase

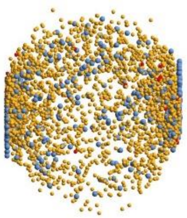

- ❑ **Initial A+A collisions :**
  N+N → string formation → decay to pre-hadrons + leading hadrons

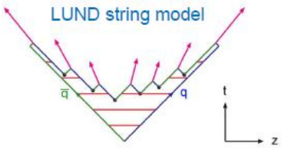

- ❑ **Formation of QGP stage if local $\varepsilon > \varepsilon_{critical}$:**
  dissolution of pre-hadrons → partons

- ❑ **Partonic phase - QGP:**
  QGP is described by the Dynamical QuasiParticle Model (DQPM) matched to reproduce lattice QCD EoS for finite T and μ_B (crossover)

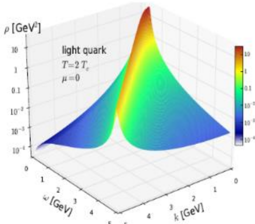

  - Degrees-of-freedom: strongly interacting quasiparticles: massive quarks and gluons (g,q,q_{bar}) with sizeable collisional widths in a self-generated mean-field potential

  - Interactions: (quasi-)elastic and inelastic collisions of partons

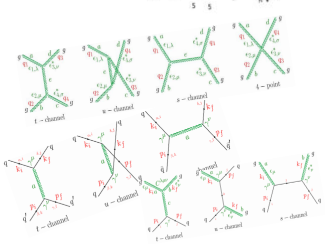

- ❑ **Hadronization to colorless off-shell mesons and baryons:**
  Strict 4-momentum and quantum number conservation

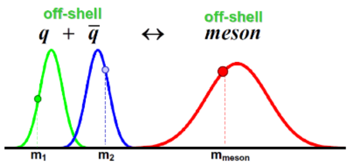

- ❑ **Hadronic phase: hadron-hadron interactions – off-shell HSD**

W. Cassing, E. Bratkovskaya, PRC 78 (2008) 034919; NPA831 (2009) 215; W. Cassing, EPJ ST 168 (2009) 3

Extraction of (T, μ_B) in PHSD

- **For each cell in PHSD :**
  In order to extract (T, μ_B) use lQCD relations (up to 4th order) - Taylor series :

(1)
lQCD

$$\begin{cases} \dfrac{n_B}{T^3} \approx \chi_2^B(T)\left(\dfrac{\mu_B}{T}\right) + \cdots \\ \Delta\epsilon/T^4 \approx \dfrac{1}{2}\left(T\dfrac{\partial \chi_2^B(T)}{\partial T} + 3\chi_2^B(T)\right)\left(\dfrac{\mu_B}{T}\right)^2 + \cdots \end{cases}$$

*** Use baryon number susceptibilities χ_n from lQCD**

➔ **obtain (T, μ_B) by solving the system of coupled equations using ε^{PHSD} and n_B^{PHSD}**

*** Done by the Newton-Raphson method**

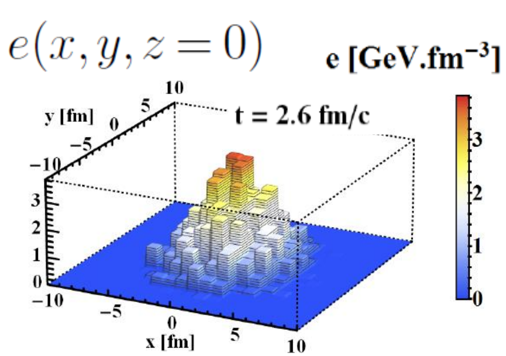

Input:

ε^{PHSD} and n_B^{PHSD}

(1)
→
lQCD

Output:

T, μ_B

P. Moreau et al., PRC100 (2019) 014911

Illustration for a HIC ($\sqrt{s_{NN}} = 19.6$ GeV)

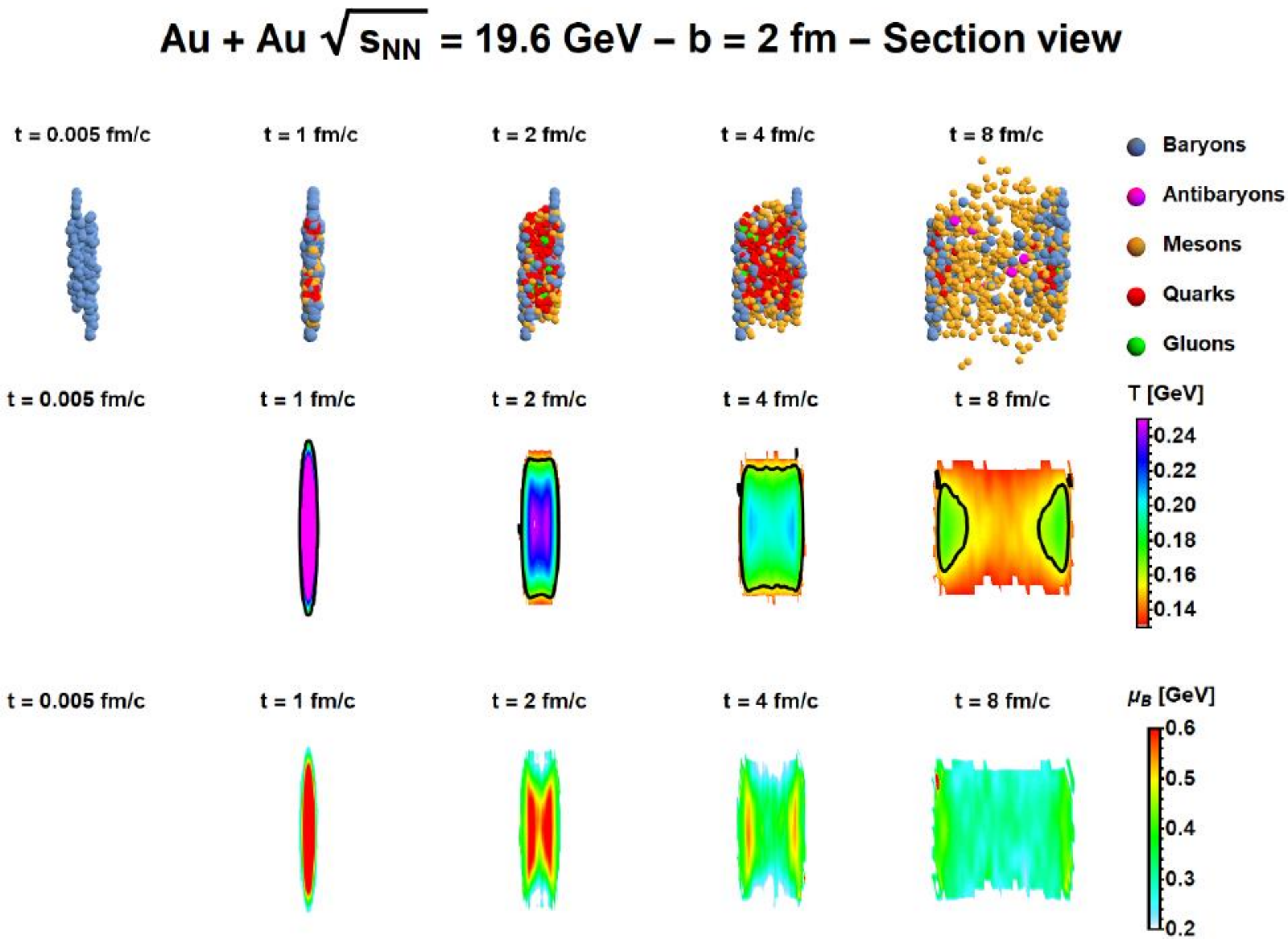

P. Moreau, PhD Thesis, Frankfurt, 2019

Illustration for a HIC ($\sqrt{s_{NN}} = 17$ GeV)

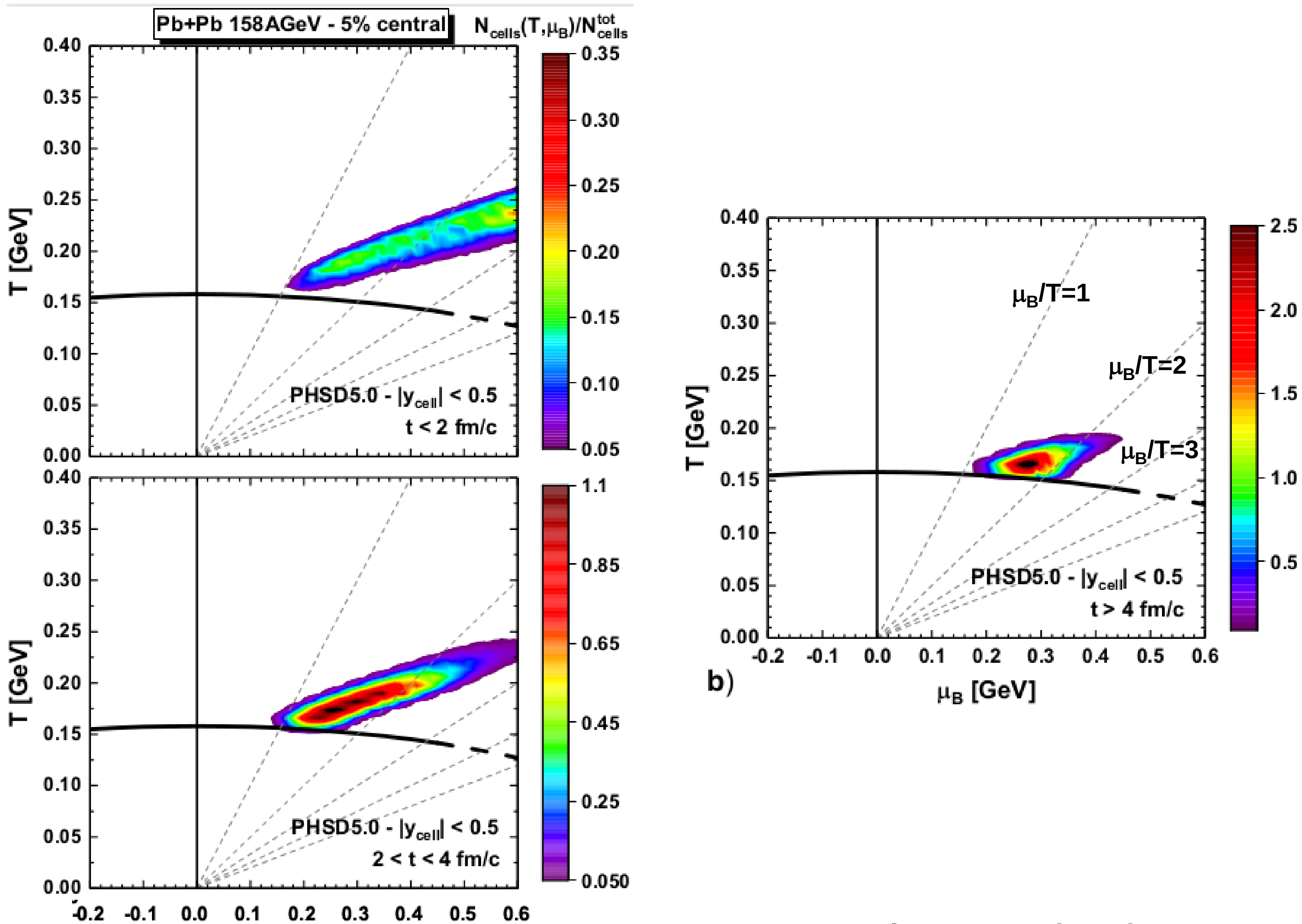

P. Moreau et al., PRC100 (2019) 014911

Traces of the QGP **at finite μ_q** in observables
in high energy heavy-ion collisions

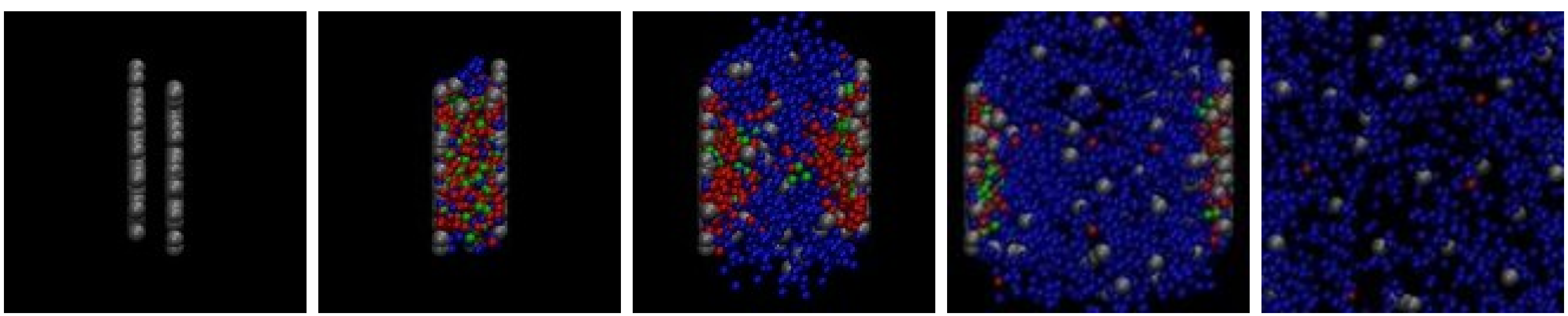

Results for HICs with PHSD 4.0 and 5.0

- **Comparison between three different results:**

1) PHSD 4.0 : only $\sigma(T)$ and $\rho(T)$

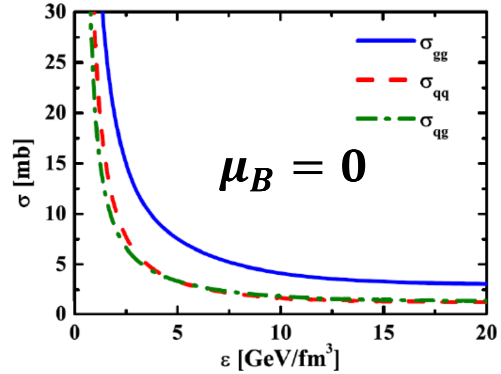

$\sigma(T)$ – parton interaction cross sections
$\rho(T)$ – spectral function of partons
➔ (masses and widths)

2) PHSD 5.0 : with $\sigma\left(\sqrt{s}, m_1, m_2, T, \underline{\mu_B = 0}\right)$ and $\rho(T, \mu_B = 0)$

In v.5.0: + angular dependence of diff. partonic cross sections

3) PHSD 5.0 : with $\sigma\left(\sqrt{s}, m_1, m_2, T, \mu_B\right)$ and $\rho\,(T, \mu_B)$

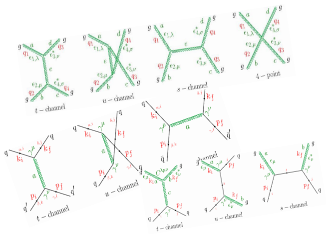

P. Moreau et al., PRC100 (2019) 014911

Results for HICs ($\sqrt{s_{NN}} = 200$ GeV)

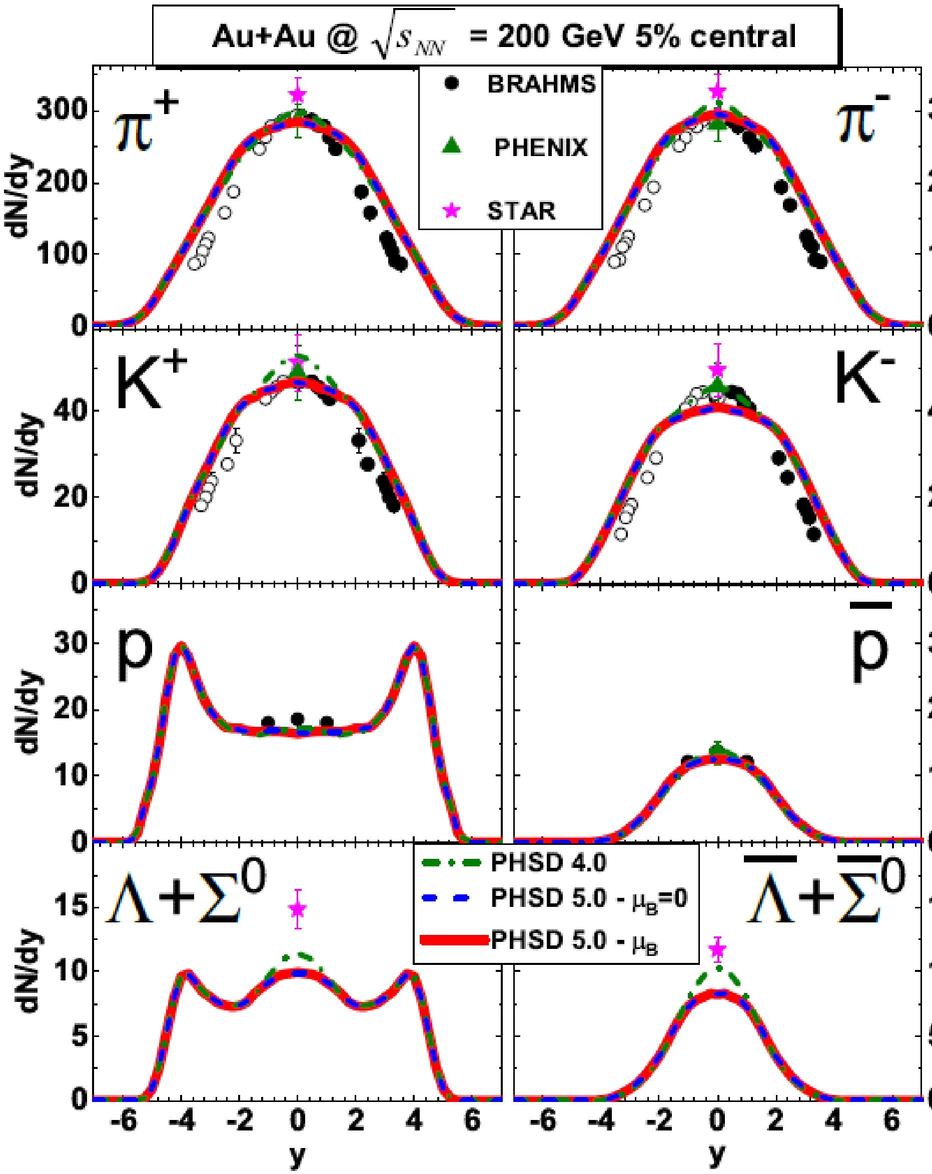

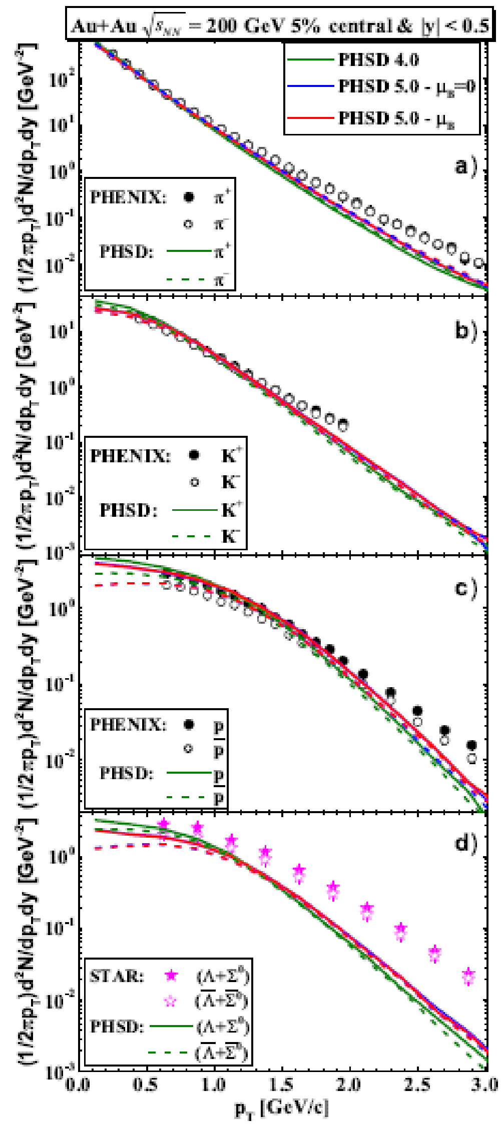

P. Moreau et al., PRC100 (2019) 014911

Results for HICs ($\sqrt{s_{NN}} = 17$ GeV)

High-μ_B regions are probed at low $\sqrt{s_{NN}}$ or high rapidity regions
But, QGP fraction is small at low $\sqrt{s_{NN}}$

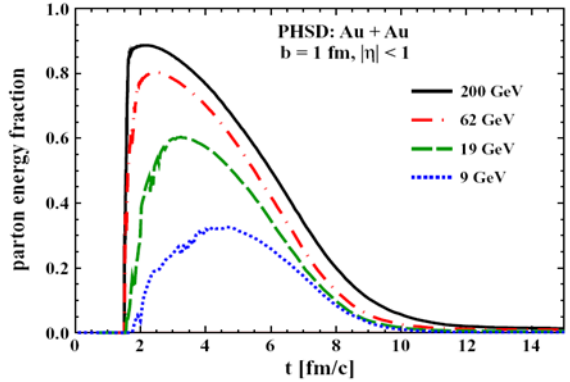

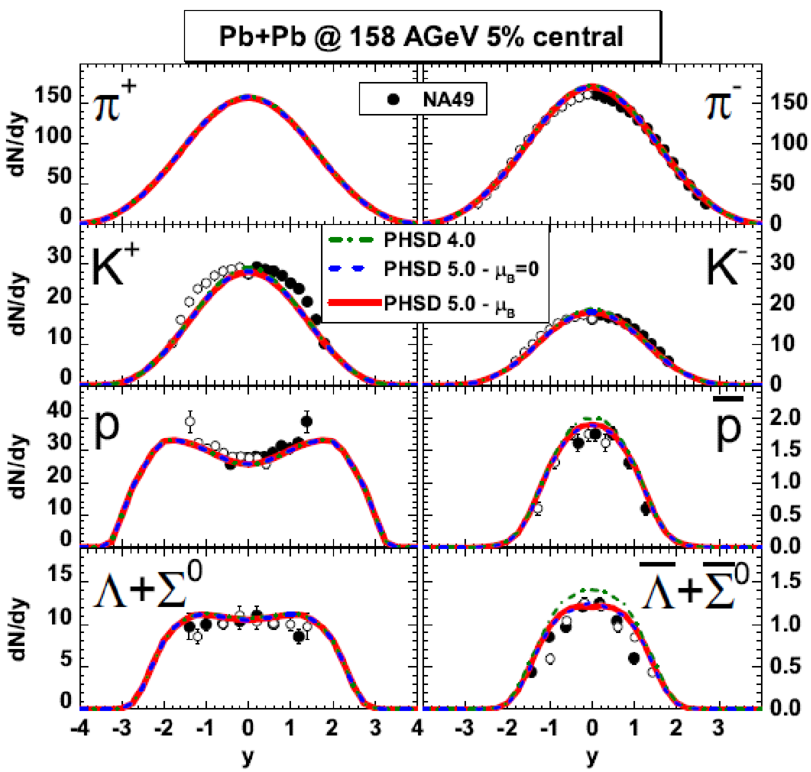

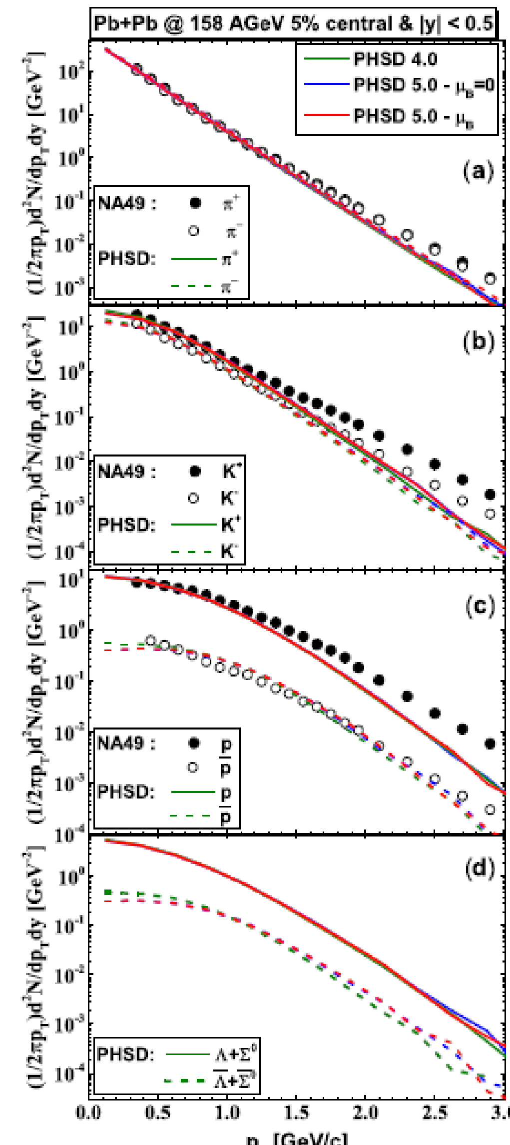

P. Moreau et al., PRC100 (2019) 014911

Results for HICs ($\sqrt{s_{NN}} = 7.6$ GeV)

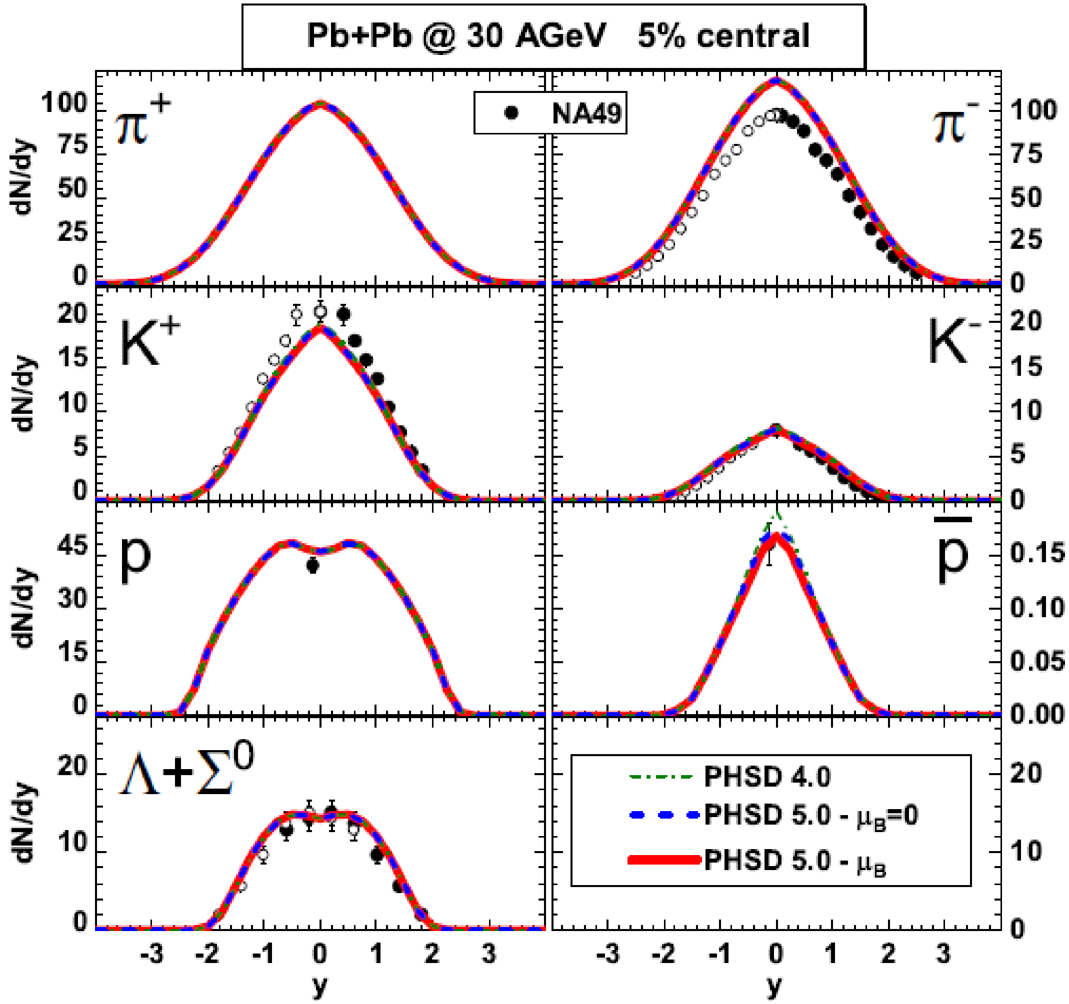

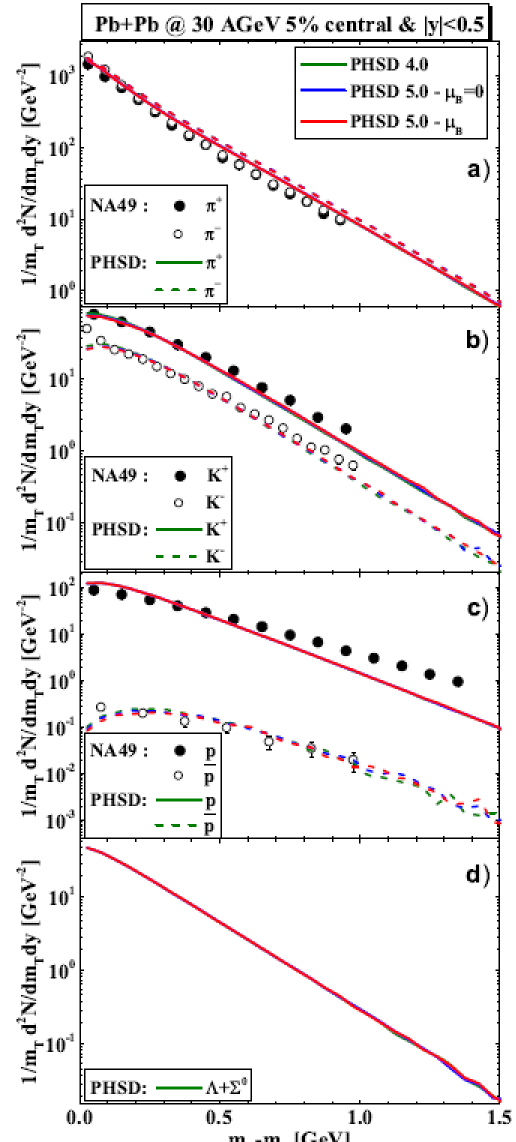

- very weak dependence of ‘bulk’ observables on μ_B

P. Moreau et al., PRC100 (2019) 014911

Results for HICs ($\sqrt{s_{NN}} = 4.86$ GeV)

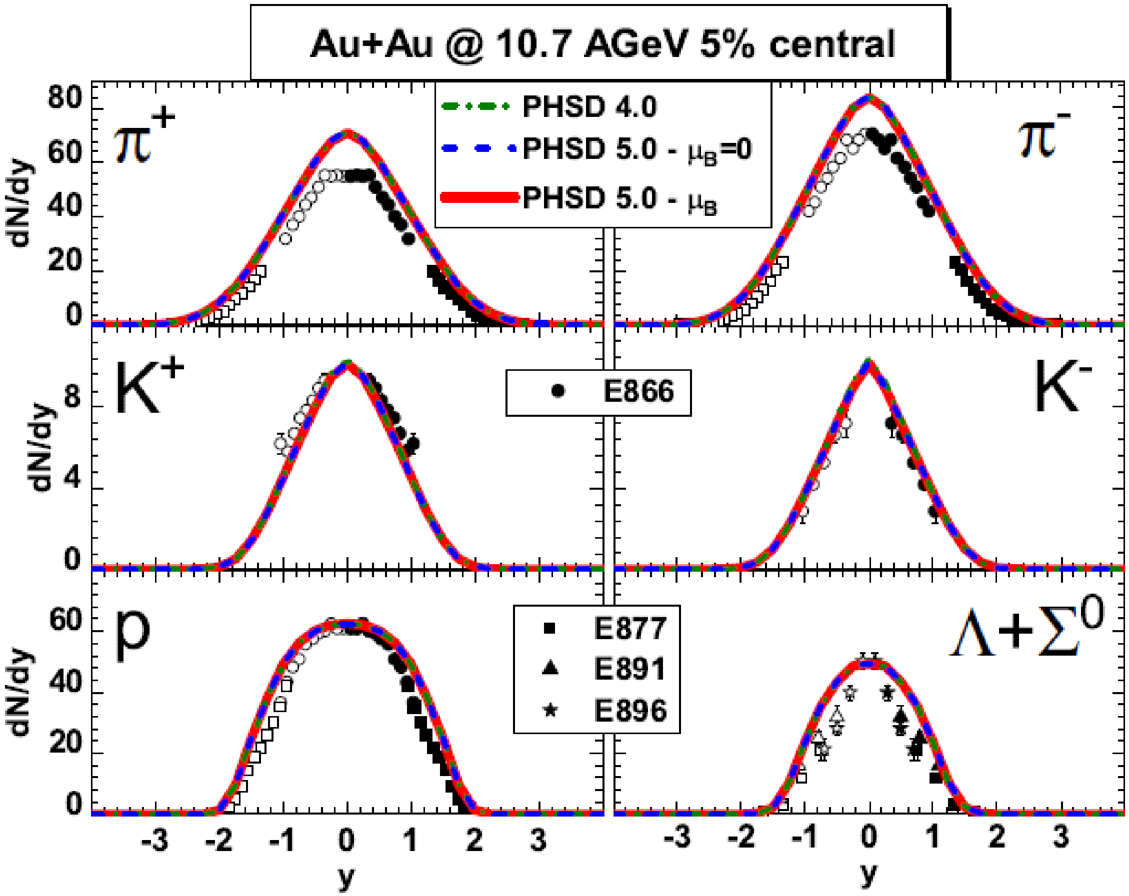

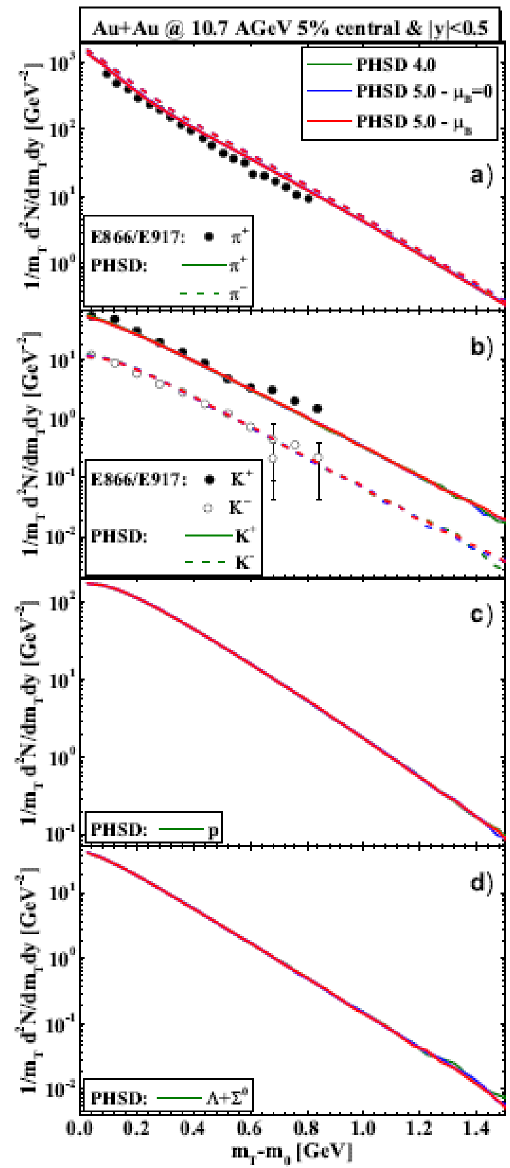

- very **weak dependence** of 'bulk' observables on μ_B

P. Moreau et al., PRC100 (2019) 014911

Elliptic flow v_2 ($\sqrt{s_{NN}} = 200\ GeV\ vs\ 27GeV$)

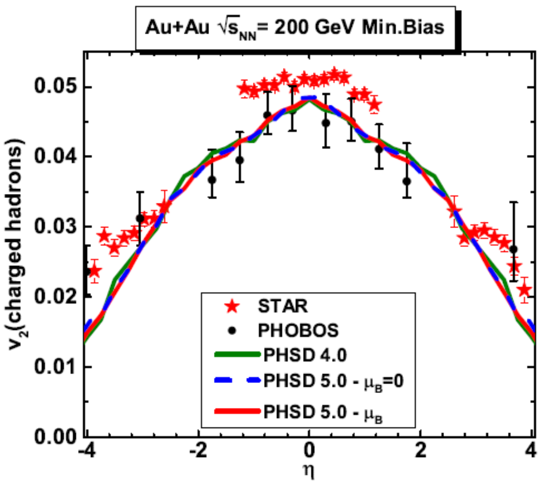

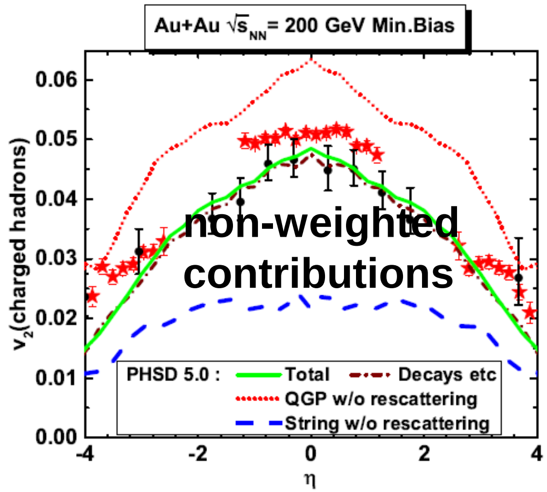

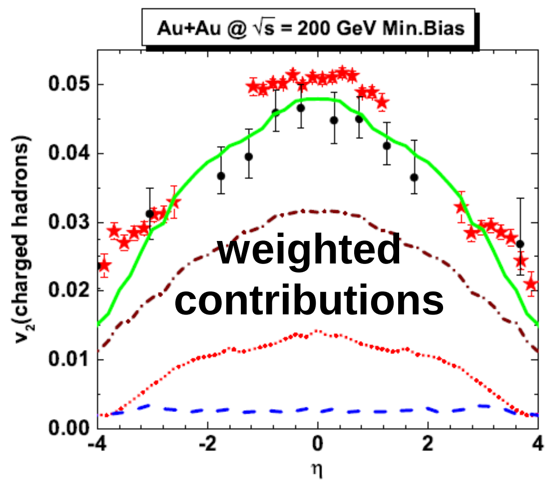

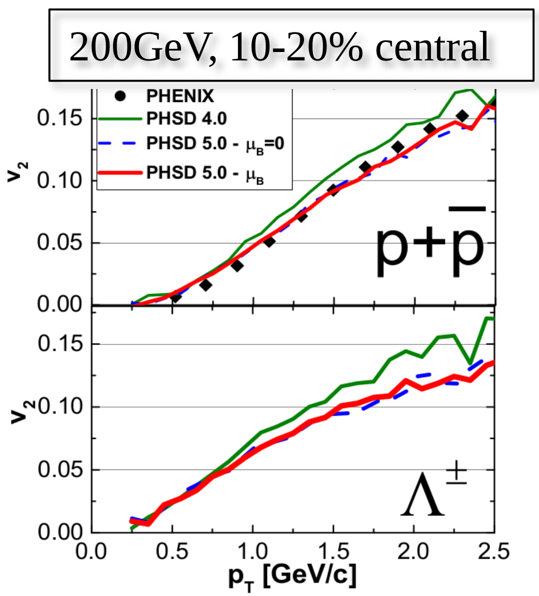

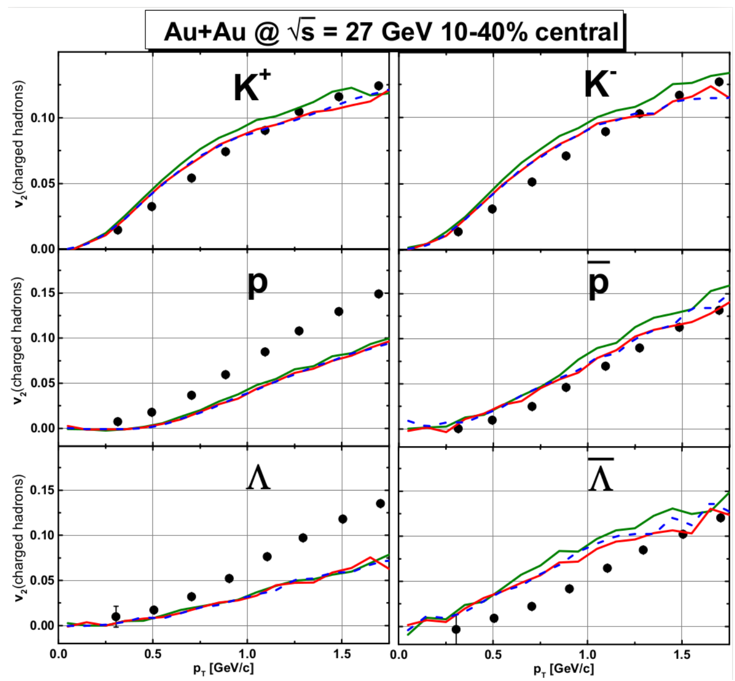

➔ **Small effect of μ_B dependence on v_2**

O. Soloveva et al., arXiv:2001.07951, MDPI Particles 2020, 3, 178

Results for v_1 for HICs ($\sqrt{s_{NN}} = 27$ GeV)

v_1

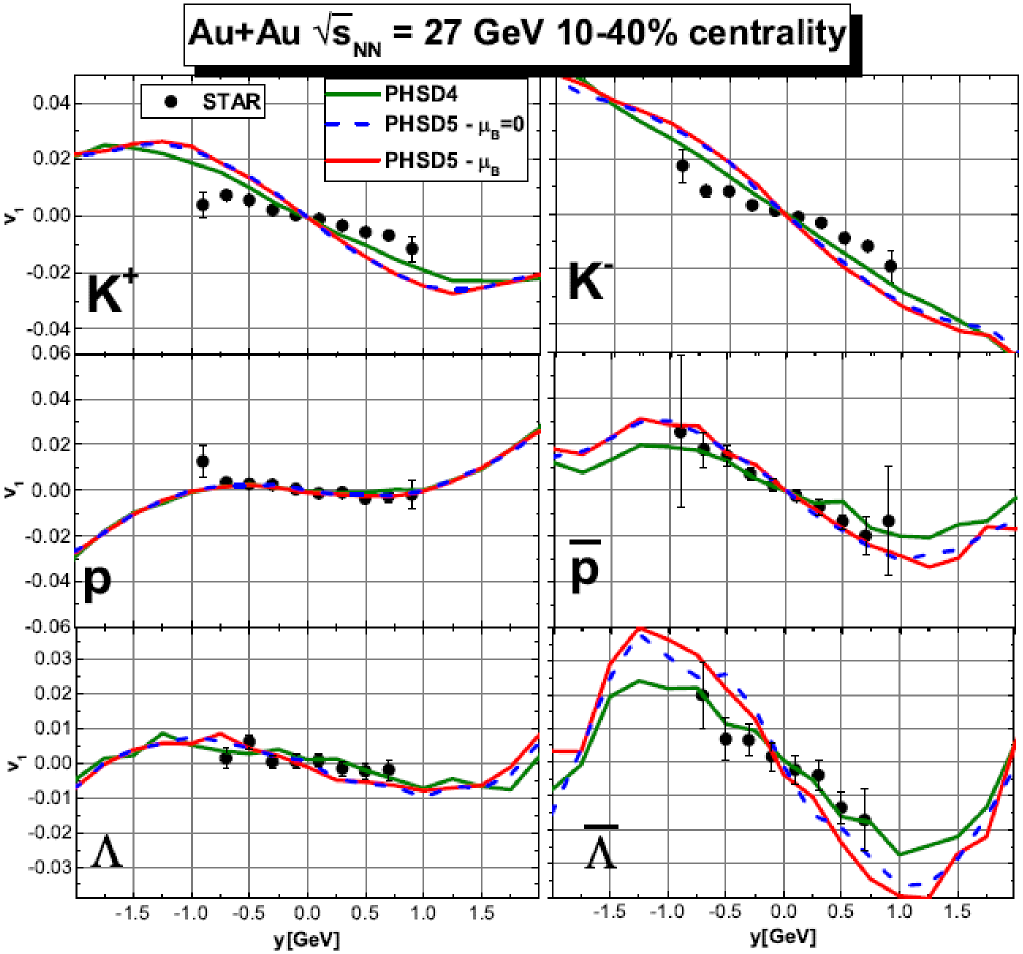

v_1, v_2 analysis:

- **weak dependence** of v_1, v_2 on μ_B
- **small influence** on v_1, v_2 of explicit $\sqrt{s}$ **-dependence** of total partonic cross sections σ + **angular dependence** of dσ/dcosθ due to the relatively **small QGP volume**
- strong **flavor dependence** of v_1, v_2

O. Soloveva et al., arXiv:2001.07951, MDPI Particles 2020, 3, 178

Summary / Outlook

- (T, μ_B)-dependent partonic cross sections and masses/widths of quarks and gluons have been implemented in PHSD
- High-μ_B region is probed at low bombarding energies or high rapidity regions
- But, QGP fraction is small at low bombarding energies:
  ➔ no effects of (T, μ_B)-dependent partonic cross sections and masses/widths seen in 'bulk' observables – dN/dy, p_T-spectra
- Flow harmonics v_1, v_2 show :
  visible sensitivity to the explicit $\sqrt{s}$ -dependence of total partonic cross sections σ + angular dependence of dσ/dcosθ, however, weak dependence on μ_B

Outlook:

- More precise EoS at large μ_B
- Possible 1st order phase transition at even larger μ_B?!

High-μ_B region of QCD phase diagram ➔ challenge for FAIR, NICA, BES RHIC